Astron. Astrophys. 329, 443–450 (1998)

ASTRONOMY
AND
ASTROPHYSICS

Dense gas in nearby galaxies

XI. Interstellar $^{12}C/^{13}C$ ratios in the central regions of M 82 and IC 342⋆

C. Henkel[1], **Y.-N. Chin**[2,3], **R. Mauersberger**[4], **and J.B. Whiteoak**[5,6]

[1] Max-Planck-Institut für Radioastronomie, Auf dem Hügel 69, D-53121 Bonn, Germany
[2] Institute of Astronomy and Astrophysics, Academia Sinica, P.O.Box 1-87 Nankang, 115 Taipei, Taiwan
[3] Radioastronomisches Institut der Universität Bonn, Auf dem Hügel 71, D-53121 Bonn, Germany
[4] Steward Observatory, The University of Arizona, Tucson, AZ 85721, USA
[5] Australia Telescope National Facility, Radiophysics Laboratories, P.O. Box 76, Epping, NSW 2121, Australia
[6] Paul Wild Observatory, Australia Telescope National Facility, CSIRO, Locked Bag 194, Narrabri NSW 2390, Australia

Received 9 September 1996 / Accepted 21 July 1997

Abstract. $^{12}C/^{13}C$ line intensity ratios have been derived from several carbon-bearing molecules to confine the range of carbon and oxygen isotope abundance ratios toward the nuclear regions of two infrared bright galaxies. The most stringent limits are obtained from CN mm-wave emission lines. Supplementary measurements toward the Galactic center region indicate that overall $I(^{12}CN)/I(^{13}CN)$ line intensity ratios are giving lower limits to the corresponding $^{12}C/^{13}C$ abundance ratio. Toward M 82 and IC 342, we find $^{12}C/^{13}C > 40$ and >30. Therefore the smaller $^{12}C/^{13}C$ ratio of our own Galactic center region (25) may not be typical for central regions of galaxies which are more luminous in the infrared. The $^{12}C/^{13}C$ limits and data from various isotopic species of CO also infer $^{16}O/^{18}O$ abundance ratios of > 90 and > 125 for M 82 and IC 342, respectively. From the $I(HC^{14}N)/I(HC^{15}N)$ line intensity ratio, $^{14}N/^{15}N > 100$ is derived for M 82.

Key words: ISM: abundances – galaxies: abundances – radio lines: ISM – radio lines: galaxies

1. Introduction

Isotope ratios derived from CNO elements have significantly contributed to our understanding of the nuclear processing in stars and the 'chemical' evolution of galaxies, since these elements are abundant and have stable 'primary' and 'secondary' nuclei. From a theoretical point of view, $^{12}C/^{13}C$ is the least controversial CNO isotope ratio: ^{12}C is a 'primary' product of helium-burning, ^{13}C is mainly a 'secondary' product of hydrogen-burning with ^{12}C as the seed nucleus. Some primary ^{13}C may also be synthesized during the third dredge up in stars of intermediate mass ('hot bottom burning', e. g. Renzini & Voli 1981).

There is evidence for high $^{12}C/^{13}C$ ratios in the central regions of active star-forming galaxies with high luminosities in the far infrared (for a summary, see Henkel & Mauersberger 1993). First hints were obtained from distant mergers (being ultraluminous in the infrared) which were showing integrated $I(^{12}CO)/I(^{13}CO)$ J=1–0 line intensity ratios >20 (Aalto et al. 1991; Combes et al. 1991; Casoli et al. 1992a,b). An interpretation in terms of an extended halo of weak ^{12}CO and negligible ^{13}CO emission is not supported by a comparison of filled-aperture with interferometric CO data (P.M. Solomon, priv. comm.). The generally accepted explanation involves inflow of disk gas with high $^{12}C/^{13}C$ ratios into the central region, possibly combined with a ^{12}C enhancement caused by nucleosynthesis in massive stars. Most direct evidence for high $^{12}C/^{13}C$ ratios was obtained from recent studies of the central regions of the nearby starburst galaxies NGC 253 and NGC 4945; this is based on $^{12}C/^{13}C$ line intensity ratios from a variety of molecular species (Henkel et al. 1993, 1994). The estimated $^{12}C/^{13}C$ abundance ratios, 40 – 50, are larger than the value for the central region of the Milky Way, ~ 25 (e. g. Wilson & Rood 1994).

Since two well studied extragalactic sources represent too small a sample for a comparison with the Milky Way, we have extended this list, including M 82 (NGC 3034) and IC 342. These contain powerful far infrared sources in their central regions and show an impressive amount of strong molecular lines (e. g. Henkel et al. 1986, 1991). From our experience with NGC 253, the best limits to the $^{12}C/^{13}C$ abundance ratio are obtained from the $I(^{12}CN)/I(^{13}CN)$ line intensity ratios. We observed CN not only toward M 82 and IC 342 but also toward the Galactic center region (see Table 1), where the interstellar $^{12}C/^{13}C$ ratio is known and where isotope ratios deduced from CN can thus be tested.

Send offprint requests to: C. Henkel, p220hen@mpifr-bonn.mpg.de

⋆ Based on observations with the IRAM 30-m telescope, Pico Veleta, Spain and the Swedish-ESO Submillimetre Telescope (SEST) at the European Southern Observatory (ESO), La Silla, Chile

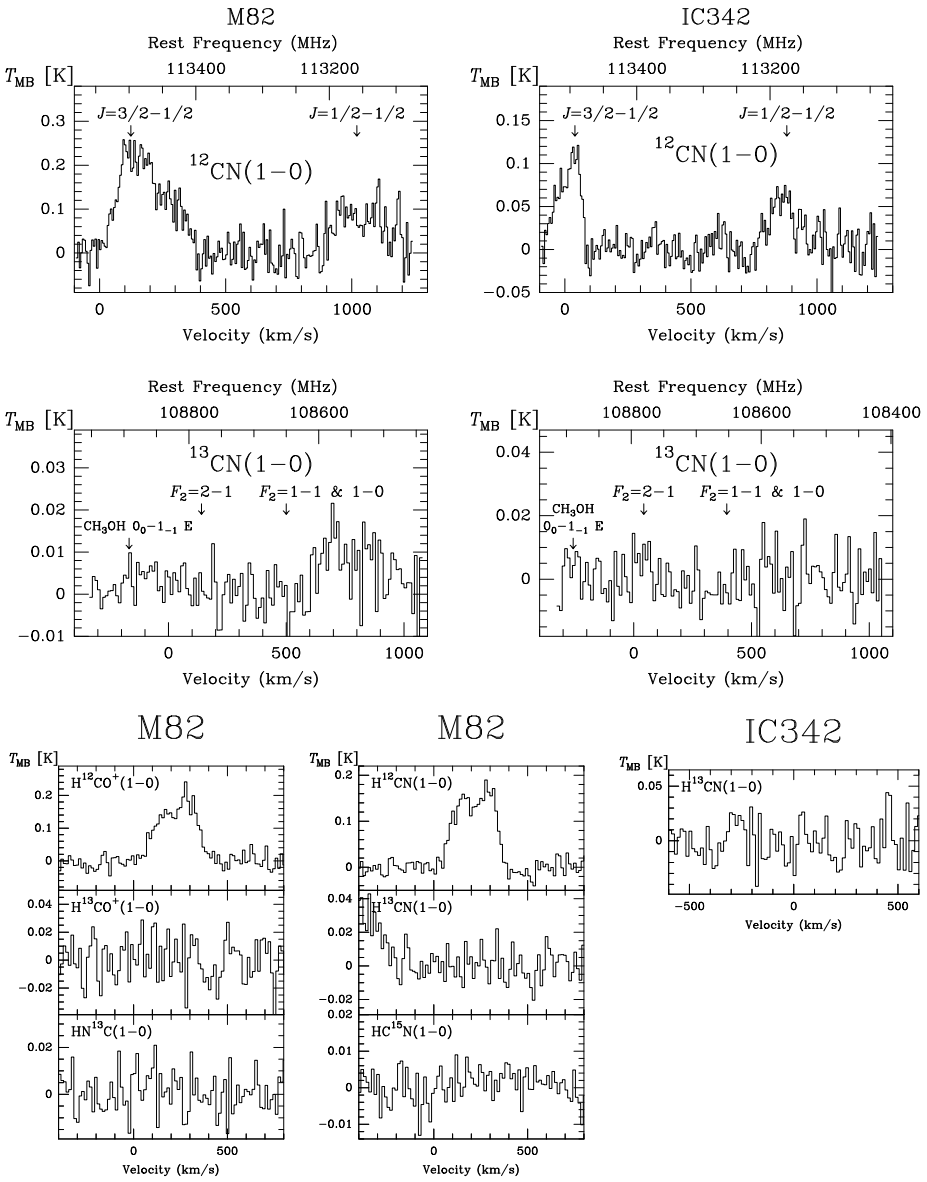

Fig. 1. Observed spectra of molecules and their ^{13}C-bearing isotopic species toward M 82 and IC 342. The spectra are smoothed to a channel spacing of 4 MHz ($\sim$ 12 km s^{-1}).

2. Observations

2.1. 30-m IRAM telescope

Observations of CN, HCN, HCO$^+$, and HNC (for frequencies, see Tables 2 and 3) were made toward the central regions of M 82 and IC 342 in June 1993 using the IRAM 30-m telescope (Baars et al. 1987) on Pico Veleta, Spain. Between 86 and 113 GHz the full width to half power beam size was 26″ – 22″. An SIS receiver was employed with system temperatures of $\sim$ 500 K on a main beam brightness temperature ($T_{\rm MB}$; e. g. Downes 1989) scale. The λ = 3 mm main beam efficiency was $\eta_{\rm MB} \sim 0.60$ As backend an 864 channel acousto-optical spectrometer (AOS) with a channel spacing of 0.58 MHz was used for ^{12}CN. A 512×1 MHz filterbank was used for ^{13}CN, H^{12}CO$^+$, H^{13}CO$^+$, H^{12}CN, H^{13}CN, HC^{15}N, and HN^{13}C, respectively. The 'channel spacing' ($\sim$ 90% of the 'channel resolution') corresponds to a velocity separation of 1.5 km s^{-1} for the ^{12}CN N=1–0 transition and 2.8 – 3.5 km s^{-1} for the other lines. The spectra were obtained with a wobbling secondary mirror using a switch cycle of four seconds (2 s on source, 2 s off-source) and a beam throw of 200″ – 240″ in azimuth. The pointing accuracy, based on nearby continuum sources and the lineshape of the simultaneously measured ^{12}CO(2–1) feature, was $\sim$ 5″or better.

All data were calibrated by observing a cold load at liquid nitrogen temperature and a chopper wheel at ambient temperature. The receivers were tuned to a single sideband mode with an image sideband rejection of typically 7 dB. The image sideband rejection was determined with a signal generator, inducing lines at the signal and image sideband frequencies about one or two days prior to the start of the observations. During the observations line intensities were regularly monitored toward Orion-KL and IRC+10216. These remained stable to within 10 – 15% of the values given by Mauersberger et al. (1989).

Table 1. Source list

Object	Distance	α_{1950} [h m s]	δ_{1950} [° ′ ″]	$v_{\rm LSR}$ [km s^{-1}]
IC 342	1.8 Mpc	3 41 57.5	67 56 40	40
M 82	3.3 Mpc	9 51 43.0	69 55 00	180
M−013−008	8.5 kpc	17 42 26.5	−29 04 10	15
M−002−007	8.5 kpc	17 42 40.0	−28 58 14	50
M+007−008	8.5 kpc	17 42 55.3	−28 53 57	50
M+011−008	8.5 kpc	17 43 01.1	−28 51 55	50

2.2. 15-m SEST

The measurements toward the Galactic center region were made in May 1994 using the 15-m Swedish-ESO Submillimetre Telescope (SEST; Booth et al. 1989) at La Silla, Chile. At the frequencies of the N=1–0 transitions of ^{12}CN and ^{13}CN the beamwidth was $\sim 45''$. The main-beam efficiency was $\eta_{\rm MB}$ = 0.70. We employed a Schottky receiver (which was sensitive to only one sideband) with system temperatures of order 500 K on a $T_{\rm MB}$ temperature scale. The image sideband rejection was $\sim$ 15 dB. The backend was an acousto-optical spectrometer with 1600 contiguous channels and a channel separation of 0.68 MHz (1.8 – 1.9 km s^{-1}). All measurements were carried out in position-switching mode. The reference position ($l^{\rm II}$,$b^{\rm II}$) = (0′,+720′) was checked to have no emission down to a 3σ level of $T_{\rm MB}$ = 50 mK. No absorption, caused by emission from the off-positions, was seen in any of the Galactic center spectra. Integration times varied from 1 minute for ^{12}CN to 20 minutes for ^{13}CN.

The pointing accuracy, obtained from measurements of SiO maser sources, was better than 10″. The stability of the 3 mm Schottky receiver was examined by comparing C^{34}S and C^{33}S spectra from Orion-KL, taken in September 1993, May 1994, and January 1995; the line temperatures are consistent within 15%.

3. Results

Distances, coordinates, and radial velocities of the observed sources are displayed in Table 1. All data were converted to a $T_{\rm MB}$ scale and first order baselines were subtracted. The CN line parameters can be found in Table 2. Fig. 1 displays the spectra obtained toward the nuclear regions of M 82 and IC 342. Toward these extragalactic sources, the ^{12}CN hyperfine components (see Sect. 4.1) are not resolved and only two broad features are seen. ^{13}CN was not detected. The broad feature in the ^{13}CN spectrum of M 82 (rest frequency either 108.58 (signal sideband) or 111.82 GHz (image sideband) for $v_{\rm LSR} \sim 180$ km s^{-1}) remains unidentified. While IC 342 has also been observed in HCN J=1–0, M 82 has been observed additionally in the J=1–0 transitions of HCO$^+$, HCN, and HNC. A summary of line intensities, including a first HC^{15}N spectrum from M82, can be found in Table 3.

^{12}CN(N=1–0) and ^{13}CN(N=1–0) spectra toward sources in the Galactic center region are shown in Fig. 2. The hyperfine structure of the ^{12}CN N=1–0 J=3/2–1/2 spin-doublet line cannot be resolved, but it is no problem to resolve the hyperfine components of the N=1–0 J=1/2–1/2 transition (for details on fine structure and hyperfine splitting, see Sect. 4.1). For ^{13}CN, the low resolution AOS can resolve the N=1–0 hyperfine components from the Galactic center region into two groups. While one contains all the F_1=1 F_2=2–1 transitions, the other includes the F_1=1 F_2=1–1 and F_1=0 F_2=1–0 transitions. The F_1=1 F_2=0–1 transitions are weaker and remain undetected.

4. Discussion

The most stringent limits on ^{12}C/^{13}C isotope ratios can be deduced from CN (see Tables 2 and 3). So far, little is known on CN emission from the central region of the Milky Way, which may serve as a model of what to expect in nuclear regions of other galaxies. In the following we thus analyse the Galactic center CN data (Sect. 4.1); in Sect. 4.2 we will then combine these results with those from other molecular species to derive isotope ratios in M 82 and IC 342.

4.1. LTE deviations in ^{12}CN *and* ^{13}CN

Each ^{12}CN rotational energy level with $N > 0$ is split into a doublet by spin-rotation interaction. Because of the spin of the nitrogen nucleus (I_1 = 1), each of these components is further split into a triplet of states. The ^{13}CN energy level scheme is further complicated by the spin of the ^{13}C (I_2 = 1/2) nucleus. The calculated frequencies and relative intensities of the resulting hyperfine components are given by Skatrud et al. (1983) and Bogey et al. (1984).

In order to derive CN optical depths and column densities, we can compare the line intensity ratios of various components observed with those expected in the optically thin case under conditions of Local Thermodynamic Equilibrium (LTE). If LTE holds, line saturation leads via

$$\frac{T_{\rm MB,1}}{T_{\rm MB,2}} = \frac{1-{\rm e}^{-\tau_1}}{1-{\rm e}^{-\tau_2}} \qquad (1)$$

to line intensity ratios which are intermediate between those in the optically thin case and unity. $T_{\rm MB,i}$ is the observed main beam brightness temperature and $\tau_{\rm i}$ is the optical depth of hyperfine component i. Previous ^{12}CN N=1–0 observations of dark clouds and star-forming regions of the Galactic disk (e. g. Turner & Gammon 1975; Churchwell 1980; Churchwell & Bieging 1982, 1983; Crutcher et al. 1984) did not provide strong evidence for non-LTE effects.

For optically thin emission under conditions of LTE,

$$R_{12}\,(^{12}{\rm CN}\ N=1-0) = \frac{I(J=1/2-1/2)}{I(J=3/2-1/2)} = 0.50, \qquad (2)$$

where I is the intensity of a given line. Our observational data from the Galactic center region (Table 4), with R_{12} being typi-

Table 2. ^{12}CN to ^{13}CN ratio toward sample in the Galactic center, M 82, and IC 342.

Object	Molecule & Transition	Frequency [GHz]	$\int T_{\rm MB}\,{\rm d}v$ [K km s^{-1}]		$\frac{I(^{12}{\rm CN})}{I(^{13}{\rm CN})}$
M 82	^{12}CN N=1–0 { J=3/2–1/2	$\sim$ 113.491	52.3 ±5.8	} 74.7 ± 6.9	> 42
	^{12}CN N=1–0 { J=1/2–1/2	$\sim$ 113.180	22.4 ±3.6		
	^{13}CN N=1–0	$\sim$ 108.720		< 1.8 [a]	
IC 342[b]	^{12}CN N=1–0 { J=3/2–1/2	$\sim$ 113.491	11.2 ±2.3	} 18.9 ± 2.4	> 31
	^{12}CN N=1–0 { J=1/2–1/2	$\sim$ 113.180	7.71±0.73		
	^{13}CN N=1–0	$\sim$ 108.720		< 0.61 [a]	
M-013-008	^{12}CN N=1–0 { J=3/2–1/2 [c]	$\sim$ 113.491	56.5 ±1.1	} 123 ± 1.8	15.0 ± 0.9
	^{12}CN N=1–0 { J=1/2–1/2 F=3/2–3/2	113.191	14.4 ±0.7		
	^{12}CN N=1–0 { J=1/2–1/2 F=3/2–1/2	113.171	23.6 ±0.7		
	^{12}CN N=1–0 { J=1/2–1/2 F=1/2–3/2	113.144	16.6 ±0.7		
	^{12}CN N=1–0 { J=1/2–1/2 F=1/2–1/2	113.123	12.3 ±0.8		
	^{13}CN N=1–0 { F_2=2–1	$\sim$ 108.720	2.75±0.22	} 8.2 ± 0.4	
	^{13}CN N=1–0 { F_2=1–1 & F_2=1–0	$\sim$ 108.654	5.47±0.29		
M-002-007	^{12}CN N=1–0 { J=3/2–1/2 [c]	$\sim$ 113.491	104 ±0.7	} 189 ± 1.1	9.4 ± 0.3
	^{12}CN N=1–0 { J=1/2–1/2 F=3/2–3/2	113.191	26.1 ±0.5		
	^{12}CN N=1–0 { J=1/2–1/2 F=3/2–1/2	113.171	30.8 ±0.4		
	^{12}CN N=1–0 { J=1/2–1/2 F=1/2–3/2	113.144	17.9 ±0.4		
	^{12}CN N=1–0 { J=1/2–1/2 F=1/2–1/2	113.123	9.66±0.39		
	^{13}CN N=1–0 { F_2=2–1	$\sim$ 108.720	9.34±0.38	} 20.0 ± 0.6	
	^{13}CN N=1–0 { F_2=1–1 & F_2=1–0	$\sim$ 108.654	10.7 ±0.4		
M+007-008	^{12}CN N=1–0 { J=3/2–1/2 [c]	$\sim$ 113.491	53.1 ±0.5	} 87.0 ± 0.8	15.0 ± 0.8
	^{12}CN N=1–0 { J=1/2–1/2 F=3/2–3/2	113.191	10.1 ±0.4		
	^{12}CN N=1–0 { J=1/2–1/2 F=3/2–1/2	113.171	13.6 ±0.3		
	^{12}CN N=1–0 { J=1/2–1/2 F=1/2–3/2	113.144	8.15±0.35		
	^{12}CN N=1–0 { J=1/2–1/2 F=1/2–1/2	113.123	2.06±0.27		
	^{13}CN N=1–0 { F_2=2–1	$\sim$ 108.720	2.65±0.16	} 5.8 ± 0.3	
	^{13}CN N=1–0 { F_2=1–1 & F_2=1–0	$\sim$ 108.654	3.14±0.19		
M+011-008	^{12}CN N=1–0 { J=3/2–1/2 [c]	$\sim$ 113.491	44.5 ±0.6	} 82.7 ± 1.0	13.1 ± 0.8
	^{12}CN N=1–0 { J=1/2–1/2 F=3/2–3/2	113.191	11.3 ±0.4		
	^{12}CN N=1–0 { J=1/2–1/2 F=3/2–1/2	113.171	13.9 ±0.4		
	^{12}CN N=1–0 { J=1/2–1/2 F=1/2–3/2	113.144	10.9 ±0.4		
	^{12}CN N=1–0 { J=1/2–1/2 F=1/2–1/2	113.123	2.20±0.32		
	^{13}CN N=1–0 { F_2=2–1	$\sim$ 108.720	2.75±0.19	} 6.3 ± 0.3	
	^{13}CN N=1–0 { F_2=1–1 & F_2=1–0	$\sim$ 108.654	3.56±0.24		

a) For undetected molecular lines, 3σ upper limits of $\int T_{\rm MB}\,{\rm d}v$ are given that are derived from the rms noise level.

b) If the tentative feature observed is not representing ^{13}CN emission, a 3 r.m.s. limit analysis corresponding to that for M 82 yields $I(^{12}{\rm CN})/I(^{13}{\rm CN}) > 31$.

c) The hyperfine components belonging to the ^{12}CN N=1–0 J=3/2–1/2 transition are not resolved in frequency.

cally slightly smaller than unity but larger than 0.5, may provide evidence for ^{12}CN line saturation. Toward M−013−008, however, a line intensity ratio of $R_{12} \sim 1.2$ hints at deviations from LTE. A detailed examination of our Galactic center data (see Table 2 and Fig. 3) provides further evidence for non-LTE effects: The J=1/2–1/2 F=3/2–3/2 feature that should be strongest among the J=1/2–1/2 spin-doublet transitions is found to be weaker than the F=3/2–1/2 component. The J=1/2–1/2 F=3/2–1/2 line is always stronger than the corresponding F=1/2–3/2 transition even though both lines should have equal strength. Another non-LTE effect can be identified when comparing the integrated intensity of the weakest resolved ^{12}CN hyperfine component, the J=1/2–1/2 F=1/2–1/2 feature, with that of the measured ^{13}CN profile. With the ^{12}CN feature only comprising 1.23% of the total CN N=1–0 intensity under optically thin LTE conditions, $I(J,F$=1/2,1/2–1/2,1/2)/$I(^{13}{\rm CN})$ line intensity ratios of 0.35 – 1.5 would yield ^{12}CN/^{13}CN abundance ratios that are well in excess of the Galactic center $^{12}{\rm C}/^{13}{\rm C}$ value.

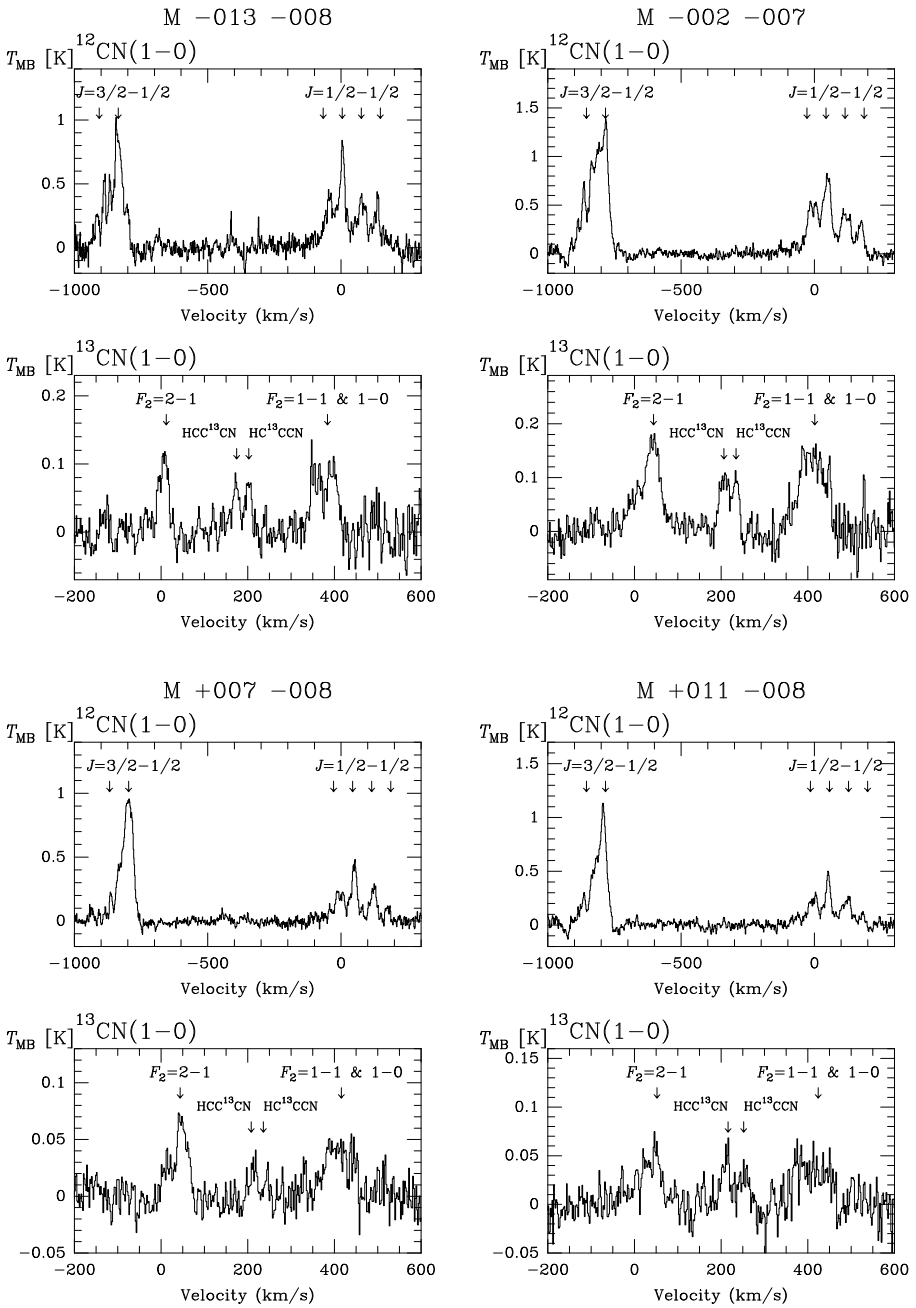

Fig. 2. Observed ^{12}CN and ^{13}CN spectra toward the Galactic center.

We conclude that lines with N=0, J,F=1/2,1/2 as lower state are enhanced relative to lines with N=0, J,F=1/2,3/2 as lower state. Apparently, N=1–0 hyperfine intensities sensitively depend on the relative populations in the N=0 doublet. A simulation infers that if the N=0, J, F=1/2,3/2 population is 'overabundant', all N=1–0 features with N=0, F, J=1/2,1/2 as lower state show enhanced line temperatures.

The low LTE intensity of the J, F=1/2,1/2–1/2,1/2 transition (1.23% of the total CN N=1–0 line strength), the discussion about fractionation given below, and the possibility to relate various LTE deviations to a single cause favor an explanation based on the relative populations of the N=0 states over alternative views, either involving optically thick ^{12}CN, N=0, J, F=1/2,1/2–1/2,1/2 lines or a high degree of isotope selective fractionation.

For ^{13}CN, the assumption of optically thin emission is very plausible. As already mentioned, ^{13}CN hyperfine components have been resolved into two main groups of transitions (Fig. 2). We can estimate the deviation from (optically thin) LTE intensity ratios by examining R_{13}, for which we obtain under LTE conditions

$$R_{13}(^{13}\mathrm{CN}\ N=1-0) = \frac{I(F_2=2-1)}{I(F_2=1-1+F_2=1-0)} = 0.83. \quad (3)$$

In Table 4 the integrated line intensity ratios in the observed Galactic center clouds are listed. Most of these ratios are, within

Table 3. Isotopic ratios from molecular observations toward M 82 and IC 342

Galaxy	Transition	$\nu_{^{12}\mathrm{CX}}$ [MHz]	$\nu_{^{13}\mathrm{CX}}$ [MHz]	$I(^{12}\mathrm{CX})$ [K km s^{-1}]	$I(^{13}\mathrm{CX})$ [K km s^{-1}]	$\frac{I(^{12}\mathrm{CX})}{I(^{13}\mathrm{CX})}$
M 82	CN(1–0)	... [a]	... [b]	74.4±6.9	< 1.8 [e]	> 42 [e]
	HCO^+(1–0)	89188.523	86754.330	44.6±1.3	< 2.4 [e]	> 19 [e]
	HCN(1–0)	88631.602	86340.184	39.6±1.0	< 1.7 [e]	> 23 [e]
	HNC(1–0)	90663.543	87090.859	13.4±0.8 [c]	< 1.6 [e]	> 9 [e]
IC 342	CN(1–0)	... [a]	... [b]	18.9±2.4	< 0.6 [e]	> 31 [e]
	HCN(1–0)	88631.602	86340.184	19.1±1.1 [d]	< 2.4 [e]	> 8 [e]
		$\nu_{\mathrm{HC^{14}N}}$ [MHz]	$\nu_{\mathrm{HC^{15}N}}$ [MHz]	$I(\mathrm{HC^{14}N})$ [K km s^{-1}]	$I(\mathrm{HC^{15}N})$ [K km s^{-1}]	$\frac{I(\mathrm{HC^{14}N})}{I(\mathrm{HC^{15}N})}$
M 82	HCN(1–0)	88631.602	86054.961	39.6±1.0	< 0.9 [e]	> 43 [e]

a) see Skatrud et al. (1983)
b) see Bogey et al. (1984)
c) HNC data from Hüttemeister et al. (1995)
d) HCN data from Nguyen-Q-Rieu et al. (1992)
e) Limits are 3 σ values.

Table 4. Line intensity ratios of ^{12}CN and ^{13}CN hyperfine components toward observed sources

Object	R_{12} [a]	R_{13} [b]
M 82	0.43±0.12	...
IC 342	0.69±0.21	...
M−013−008	1.18±0.05	0.50±0.07
M−002−007	0.81±0.01	0.87±0.07
M+007−008	0.64±0.02	0.85±0.10
M+011−008	0.86±0.03	0.77±0.11

a) R_{12} is the integrated intensity ratio of the J=1/2–1/2 to J=3/2–1/2 spin-doublet lines. In the optically thin case, the LTE value is 0.50 (see Eq. (2)).
b) R_{13} is the integrated intensity ratio of the F_1=1 F_2=2–1 to the F_1=1 F_2=1–1 and F_1=0 F_2=1–0 components. In the optically thin case under LTE conditions, the value is 0.83 (see Eq. (3)).

the 1σ error, consistent with the value from Eq. (3). The exception is M−013−008, where the ratio is 0.50 ± 0.07.

Integrating over all hyperfine components, the CN data from the Galactic center (Table 2) show that $I(^{12}\mathrm{CN})/I(^{13}\mathrm{CN})$ = 9 – 15. Based on data from a variety of sources and molecular species ($C^{18}O$, H_2CO, HCO^+, NH_2CHO, OCS; see Wannier 1980; Wilson & Rood 1994, and many references therein), there is strong evidence for an actual $^{12}C/^{13}C$ ratio of 25 ± 5 in the interstellar medium of the Galactic center region. Accounting for possible line saturation in the ^{12}CN profiles, line intensity and isotope ratios are therefore consistent. Our CN data provide *lower limits* to the $^{12}C/^{13}C$ isotope ratio and neither fractionation nor isotope selective photoionization play a dominant role.

Fractionation can be analysed in some more detail: The $^{12}CO/^{13}CO$ abundance ratio is affected by the reaction

$$^{13}C^+ + {}^{12}CO \longrightarrow {}^{12}C^+ + {}^{13}CO + \Delta E_{35\,\mathrm{K}} \quad (4)$$

(Watson et al. 1976), which enhances ^{13}CO relative to ^{12}CO and $^{12}C^+$ relative to $^{13}C^+$ in the more diffuse C^+ rich parts of molecular clouds. For ^{12}CN and ^{13}CN, the corresponding difference in the energies of the ground vibrational states is $\sim$ 32 K. While reaction (4) has little effect on the $H^{12}CO^+/H^{13}CO^+$ abundance ratio, other carbon-bearing molecules like HCN, HNC, H_2CO, and CN are affected in the sense that their $^{12}C/^{13}C$ abundance ratios follow C^+ and are thus larger than the corresponding isotope ratio (Langer et al. 1984; Langer & Graedel 1989). With $C^{18}O$ and H_2CO bracketing the actual carbon isotope ratio, observations show that these deviations must be small ($\sim$ 20 – 30% in the Galactic disk; cf. Henkel et al. 1982; Langer & Penzias 1990). In Galactic center molecular clouds T_{kin} is larger than in clouds of the disk. T_{kin} may be largest in the more active regions of IR-luminous galaxies (e. g. Mauersberger et al. 1986; Ho et al. 1990; Solomon et al. 1992) and isotope selective CN fractionation should thus be negligible.

4.2. Extragalactic isotope ratios

4.2.1. $^{12}C/^{13}C$ ratios

Our extragalactic CN data can be used to estimate $^{12}C/^{13}C$ isotope ratios, (1) because the spectra from the Galactic center region provide 'reasonable' results (see Sect. 4.1) and (2) because significant non-LTE effects are not seen in the M 82 and IC 342 spectra. The R_{12} line intensity ratios are close to the LTE value (see Eq. (2) and Table 4). Furthermore, the $HC^{13}CCN$ and $HCC^{13}CN$ features, observed in the Galactic center ^{13}CN spectra (Fig. 2), are not expected to disturb our extragalactic ^{13}CN

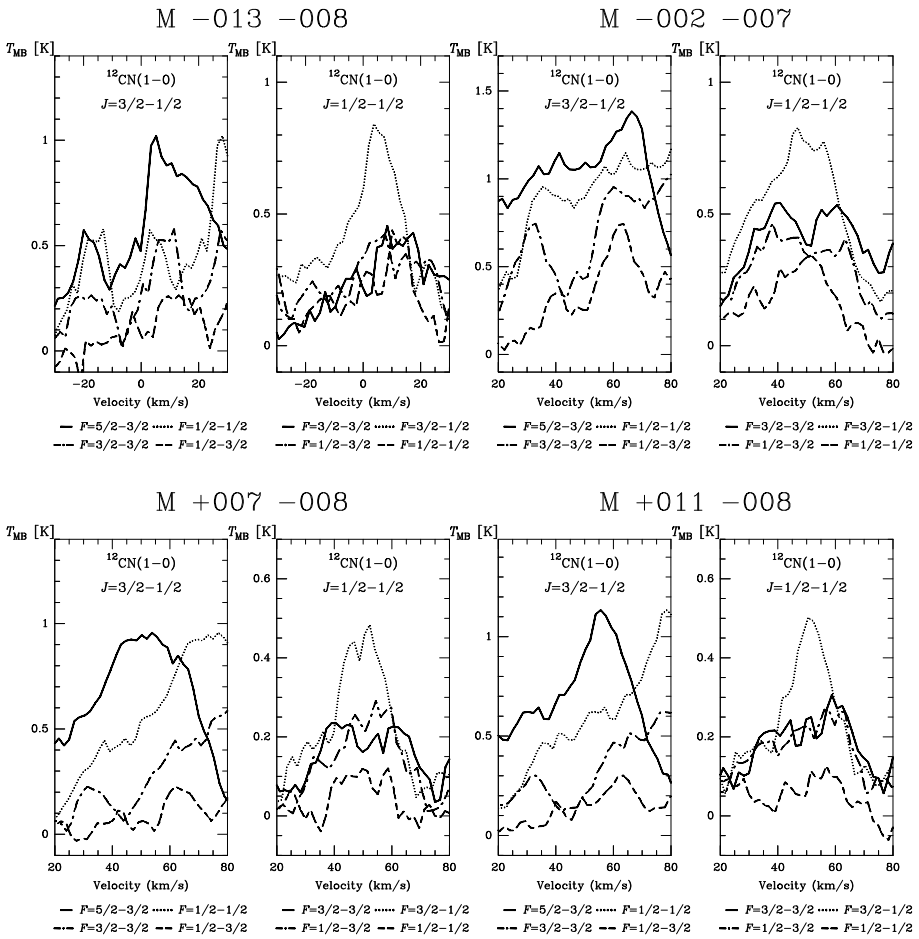

Fig. 3. Observed spectra of CN N=1–0 J=3/2–1/2 (left panel) and J=1/2–1/2 (right panel) toward the indicated clouds in the Galactic center region. All hyperfine components were obtained simultaneously in the same AOS backend; these profiles have been split and shifted by their frequency difference.

profiles: HC_3N is extremely weak in extragalactic sources (e. g. Henkel et al. 1988; Mauersberger et al. 1990). Toward our extragalactic sources, ^{12}CN is thus likely optically thin and the $I(^{12}\mathrm{CN})/I(^{13}\mathrm{CN})$ line intensity ratios of > 40 and > 30 for M 82 and IC 342, respectively, can be interpreted as lower limits to the $^{12}\mathrm{C}/^{13}\mathrm{C}$ isotope ratio.

In Table 3, lower limits to the $^{12}\mathrm{C}/^{13}\mathrm{C}$ intensity ratio are displayed for a variety of molecular species toward M 82 and IC 342. Unlike the N=1–0 CN transitions, other observed molecular lines are not significantly broadened due to hyperfine splitting. The emission from the ^{13}C-bearing isotopic species is probably optically thin, while the emission from the main species may be saturated. Since the line intensity ratio of the common ^{12}C to its rare ^{13}C-bearing isotopic species will be reduced by optical depth and self-absorption effects (this is not fully compensated by differences in excitation; see Henkel et al. 1994), the lower limit of the intensity ratio is also the lower limit to the $^{12}\mathrm{C}/^{13}\mathrm{C}$ isotopic abundance ratio.

Combining our result with previous work done toward NGC 253 and NGC 4945 (Henkel et al. 1993, 1994), a small $^{12}\mathrm{C}/^{13}\mathrm{C}$ ratio as observed in our Galactic center region appears not to be typical for galaxies with infrared luminosities similar to or higher than that of the nuclear region of the Milky Way. This result suggests (Casoli et al. 1992b) that (1) gas inflow from the outer regions adds large amounts of low-metallicity, ^{13}C-poor material to the nuclear interstellar medium or that (2) ^{12}C may be more efficiently produced (relative to ^{13}C) in regions with a high rate of massive star formation.

4.2.2. Limits to the $^{16}\mathrm{O}/^{18}\mathrm{O}$ ratio

OH and H_2CO data indicate a $^{16}\mathrm{O}/^{18}\mathrm{O}$ ratio of 250 ± 30 for the Galactic center region (e. g. Wilson & Rood 1994). Combining ^{12}CO, ^{13}CO, and $\mathrm{C}^{18}\mathrm{O}$ data with our upper limits to the $^{12}\mathrm{C}/^{13}\mathrm{C}$ ratio deduced in Sect. 4.2.1, we can also constrain the $^{16}\mathrm{O}/^{18}\mathrm{O}$ ratio. Following Henkel et al. (1994; their Sect. 6.2) and combining IRAM 30-m ^{12}CO, ^{13}CO, and $\mathrm{C}^{18}\mathrm{O}$ data from Eckart et al. (1990), Loiseau et al. (1990), Sage et al. (1991), Wild et al. (1992), and Güsten et al. (1993), we find for M 82

$$^{12}\mathrm{C}/^{13}\mathrm{C} \leq [I(^{12}\mathrm{CO})/I(^{13}\mathrm{CO}]\tau(^{12}\mathrm{CO}) \sim 17\,\tau(^{12}\mathrm{CO}) \qquad (5)$$

and

$$^{16}\mathrm{O}/^{18}\mathrm{O} \leq [I(^{12}\mathrm{CO})/I(\mathrm{C}^{18}\mathrm{O}]\tau(^{12}\mathrm{CO}) \sim 44\,\tau(^{12}\mathrm{CO}) \qquad (6)$$

and for IC 342

$$^{12}\mathrm{C}/^{13}\mathrm{C} \leq [I(^{12}\mathrm{CO})/I(^{13}\mathrm{CO}]\tau(^{12}\mathrm{CO}) \sim 11\,\tau(^{12}\mathrm{CO}) \qquad (7)$$

and

$$^{16}\mathrm{O}/^{18}\mathrm{O} \leq [I(^{12}\mathrm{CO})/I(\mathrm{C}^{18}\mathrm{O}]\tau(^{12}\mathrm{CO}) \sim 51\tau(^{12}\mathrm{CO}). \qquad (8)$$

This implies for M 82 $^{12}C/^{13}C \sim 0.39 \times (^{16}O/^{18}O)$ and for IC 342 $^{12}C/^{13}C \sim 0.22 \times (^{16}O/^{18}O)$, while for the Galactic center region, $^{12}C/^{13}C \sim 0.10 \times (^{16}O/^{18}O)$. With the lower $^{12}C/^{13}C$ limits deduced in Sect. 4.2.1 and accounting for uncertainties in the $C^{18}O$ line intensities, we thus find $^{16}O/^{18}O > 90$ and > 125 for M 82 and IC 342, respectively.

4.2.3. The $^{14}N/^{15}N$ ratio in M 82

The $^{14}N/^{15}N$ abundance ratio (270 in our solar system and ~ 400 in the local interstellar medium; e. g. Dahmen et al. 1995) has so far not been measured in an extragalactic object. According to Henkel & Mauersberger (1993), such ratios may be small ($\lesssim 150$) in nuclear starburst regions. Combining $HC^{15}N$ J=1–0 data from M 82 with HCN (i. e. $HC^{14}N$), we can derive a lower limit to the $^{14}N/^{15}N$ abundance ratio. From Table 3 a lower 3σ limit of 43 is obtained for the $I(HC^{14}N)/I(HC^{15}N)$ ratio. Estimating an $HC^{14}N$ optical depth of $\sim 3-4$ (Henkel et al. 1993), a lower limit of 43 from the $I(HC^{14}N)/I(HC^{15}N)$ intensity ratio implies that the $^{14}N/^{15}N$ isotope ratio should exceed 100.

5. Conclusions

Having studied the N=1–0 line profiles of ^{12}CN and ^{13}CN toward four Galactic center clouds and a variety of molecular species toward the central region of M 82 and IC 342, we obtain the following main results:

(1) In the Galactic center clouds, non-LTE populations in the ^{12}CN N=0 doublet lead to enhanced line intensities for hyperfine transitions with N=0, J,F=1/2,1/2 as lower state. Alternative explanations for the LTE deviations, either involving opaque J, F=1/2,1/2–1/2,1/2 lines or significant isotope selective fractionation are not attractive. No signs for line saturation or non-LTE effects are found in the CN spectra from M 82 and IC 342; non-LTE intensities in the ^{13}CN N=1–0 profile are only seen toward one Galactic center cloud, M–013–008.

(2) If line saturation affects the observed ^{12}CN features, $I(^{12}CN)/I(^{13}CN)$ line intensity ratios should be smaller than the actual $^{12}C/^{13}C$ abundance ratio, which is ~ 25 in the Galactic center region. With $I(^{12}CN)/I(^{13}CN) = 9-15$, some saturation should be present. Since $I(^{12}CN)/I(^{13}CN) \lesssim {}^{12}C/^{13}C$, we find no reason to avoid CN as a tracer to contrain $^{12}C/^{13}C$ isotope ratios in the nuclear regions of nearby galaxies.

(3) $^{12}C/^{13}C$ limits from CN are > 40 and > 30 for M 82 and IC 342, respectively. Since the $^{12}C/^{13}C$ ratios have been found to be ~ 40, ~ 50, and 25 ± 5 in NGC 253, NGC 4945, and the Galactic center region, these results are consistent with large $^{12}C/^{13}C$ ratios (>25) in the nuclear regions of starburst galaxies (M 82, NGC 253, and NGC 4945).

(4) Combining these results with measurements of various CO isotopic species, $^{16}O/^{18}O > 90$ and > 125 in M 82 and IC 342, respectively.

(5) A lower $^{14}N/^{15}N$ limit of 100 is estimated, based on an HCN J=1–0 optical depth of $\sim 3-4$ in the main species.

Acknowledgements. We thank M. Guélin for critically reading the manuscript. Y.-N. Chin thanks for financial support through DAAD (Deutscher Akademischer Austauschdienst) grant 573 307 0023 and through National Science Council of Taiwan grant 86-2112-M001-032. R. Mauersberger acknowledges support as a Heisenberg fellow by the Deutsche Forschungsgemeinschaft (DFG).

References

Aalto S., Black J.H., Johansson L.E.B., Booth R.S., 1991, A&A 249, 323
Baars J.W.M., Hooghoudt B.G., Mezger P.G., de Jonge M.J., 1987, A&A 175, 319
Bogey M., Demuynck C., Destombes J.L., 1984, Can. J. Phys. 62, 1248
Booth R.S., Delgado G., Hagström M., et al., 1989, A&A 216, 315
Casoli F., Dupraz C., Combes F., 1992a, A&A 264, 49
Casoli F., Dupraz C., Combes F., 1992b, A&A 264, 55
Churchwell E., 1980, ApJ 240, 811
Churchwell E., Bieging J.H., 1982, ApJ 258, 515
Churchwell E., Bieging J.H., 1983, ApJ 265, 216
Combes F., Casoli F., Encrenaz P., Gerin M., Laurant C., 1991, A&A 248, 607
Crutcher R.M., Churchwell E., Ziurys L.M., 1984, ApJ 283, 668
Dahmen G., Wilson T.L., Matteucci F., 1995, A&A 295, 194
Downes D., 1989, Introductory Course in Galaxies' Evolution and Observational Astronomy, eds. I. Appenzeller, H. Habing, P. Lena, Springer, Heidelberg, p353
Eckart A., Downes D., Genzel R., et al., 1990, ApJ 348, 434
Güsten R., Serabyn E., Kasemann C., et al., 1993, ApJ 402, 537
Henkel C., Mauersberger R., 1993, A&A 274, 730
Henkel C., Wilson T.L., Bieging J.H., 1982, A&A 109, 344
Henkel C., Wouterloot J.G.A., Bally J., 1986, A&A 155, 193
Henkel C., Mauersberger R., Schilke, P., 1988, A&A 201, L23
Henkel C., Baan W.A., Mauerberger R., 1991, A&AR 3, 47
Henkel C., Mauersberger R., Wiklind T., et al., 1993, A&A 268, L17
Henkel C., Whiteoak J.B., Mauersberger R., 1994, A&A 284, 17
Ho P.T.P., Martin R.N., Turner J.L., Jackson J.M., 1990, ApJ 355, L19
Hüttemeister S., Henkel C., Mauersberger R., et al., 1995, A&A 295, 571
Loiseau N., Nakai N., Sofue Y., et al., 1990, A&A 228, 331
Langer W.D., Graedel T.E., 1989, ApJS 69, 241
Langer W.D., Graedel T.E., Frerking M.A., Armentrout P.B., 1984, ApJ 277, 581
Langer W.D., Penzias A.A., 1990, ApJ 357, 477
Mauersberger R., Henkel C., Wilson T.L., Walmsley C.M., 1986, A&A 162, 199
Mauersberger R., Henkel C., Sage, L.J., 1990, A&A 236, 63
Mauersberger R., Guélin M., Martín-Pintado J., et al., 1989, A&AS 79, 217
Nguyen-Q-Rieu, Jackson J.M., Henkel C., Truong-Bach, Mauersberger R., 1992, ApJ 399, 521
Renzini A., Voli M., 1981, A&A 94, 175
Sage L.J., Mauersberger R., Henkel C., 1991, A&A 249, 31
Skatrud D.D., de Lucia F.C., Blake G.A., Sastry K.V.L.N., 1983, J. Mol. Spec. 99, 35
Solomon P.M., Downes D., Radford S.J.E., 1992, ApJ 398, L29
Turner B.E., Gammon R.H., 1975, ApJ 198, 71
Wannier P.G., 1980, ARA&A 18, 399
Watson W.D., Anichich V.G., Huntress W.T., 1976, ApJ 205, L165
Wild W., Harris A.I., Eckart A., et al., 1992, A&A 265, 447
Wilson T.L., Rood R.T., 1994, ARA&A 32, 191